

Fracture mechanics models for short crack growth estimation and fatigue strength assessment

Modelos fractomecánicos para la estimación del crecimiento de fisuras cortas y la evaluación de la resistencia a la fatiga

Mirco Daniel Chapetti¹ 

¹Consejo Nacional de Investigaciones Científicas y Técnicas – Universidad Nacional de Mar del Plata, Instituto de Investigaciones en Ciencia y Tecnología de Materiales, Laboratorio de Mecánica Experimental. Av. Colón 10850 (7600), Mar del Plata, Argentina.

e-mail: mchapetti@fi.mdp.edu.ar

ABSTRACT

The fatigue strength assessment of metallic components containing manufacturing defects is currently analysed by applying fracture mechanics-based methodologies. This work begins by dealing with the recently published paper entitled “Short crack propagation analysis and fatigue strength assessment of additively manufactured materials: an application to AISI 316L”, *Int J Fatigue* 151 (2021) 106396, by Bergant, Werner, Madia, Yawny and Zerbst, where IBESS approach and Chapetti’s short crack growth threshold models were implemented for assessing the fatigue strength of laser powder bed fusion processed AISI 316L stainless steels. The application of the Chapetti’s model is carried out here in the way its author thinks it should be made, and results show clear differences when comparing with the results of the referenced paper. Analyses of the sources of discrepancy are also carried out. Some discussions associated with other recent applications of the available fracture mechanics models and hypotheses, or their combinations, are added in order to optimize future analysis when using them for short crack growth threshold estimations. Later, several analyses are made by making general observations associated with the prediction models, their hypotheses, their combinations and their relationship to the Kitagawa-Takahashi diagram. Finally, it is shown that when applying the fracture mechanics models special attention is necessary when comparing intrinsic strengths of the analysed material and that of material-defect combinations, particularly when the defects used in the analysis are artificial and/or are relatively large comparing with the microstructural dimension.

Keywords: Fracture Mechanics; Microstructural Fatigue Threshold; Short cracks; Fatigue Strength Estimation; Small Defect Assessment.

1. INTRODUCTION

High cycle fatigue life and fatigue endurance prediction approaches for components containing defects have received increasingly more attention, especially those that are based on fracture mechanics theories [1–10]. The lifetime and fatigue strength of engineering alloys are significantly influenced by the presence of material defects and their influences can be estimated using fracture mechanics approaches.

In a recent publications Bergant and co-workers [1] have applied the Chapetti’s and the IBESS fracture mechanics-based models and approaches to analyse the fatigue behaviour of additively manufactured (AM) 316L stainless steel and the influence of small and large material defects on its fatigue endurance. The evaluation is based on two experimental data sets provided by Solberg et al. [11] and Andreau et al. [12]. The experimental data and the material properties required as input data for applying and validating the models and approaches were obtained from three literature references dealing with laser powder bed fusion processed AISI 316L stainless steels [11–13]. In the present work the same data are analysed by applying the Chapetti’s model to estimate the short crack growth threshold curve in the way the author believe that it should be applied according to available data. Results are analysed and compared with the results of the referenced paper and possible sources of discrepancy are discussed.

Later, several analyses are made by making general observations associated with the prediction models, their hypotheses, their combinations and their relationship to the Kitagawa and Takahashi (K-T) diagram. Discrepancies observed and discussed in this work show the importance of having measured data for the analysed material and the errors that can be made when using measured values from others, especially in materials produced with additive manufacturing in which the properties depend on many parameters for the same powder. Finally, it is shown that when applying the fracture mechanics models special attention is necessary when comparing intrinsic strengths of the analysed material and that of material-defect combinations, particularly when the defects used in the analysis are artificial and/or are relatively large comparing with the microstructural dimension (e.g. grain size).

2. MATERIAL AND EXPERIMENTS DATA

The analysis was (by Bergant et al. [1]) and is (in the present work) done on the experimental fatigue data reported by Solberg et al. [11] and Andraeu et al. [12]. In both studies, AM 316L stainless steel in the as-built condition produced by the Laser Powder Bed Fusion (L-PBF) technique was investigated. The experimental data taken for the analyses can be found in reference [1], [11] and [12].

Solberg et al. [11] determined the material's $\Delta\sigma$ -N curve and tests were performed under load control with a loading ratio $R = 0.1$ (runouts: 2×10^6 cycles without fracture). Cylindrical specimens with a diameter of 4.5 mm and as-built surface roughness were tested. For each test leading to failure, the location of the killer defect and its initial area was reported. Solberg's study showed that fatigue failures at higher loading levels (and smaller fatigue lives) were related to very large internal defects (in the range of sizes between 0,56 and 0,78 mm, see references [1,11]), while for lower loading levels (and longer fatigue lives), the crack nucleated at surface defects (in the range of sizes between 0,06 and 0,14 mm, see references [1,11]).

Andraeu et al. [12] analysed as-built L-PBF AM 316L specimens. Fatigue tests were performed under load control with a loading ratio $R = 0.1$ (runouts: 10^6 cycles without fracture). Machined and polished fatigue cylindrical specimens with a 3.5 mm diameter were used. Almost all the defects that nucleated the cracks that led to the fracture were located at the surface (defect sizes in the range between 0,034 and 0,087 mm, see references [1,12]).

In both cases, a long crack propagation threshold ΔK_{thR} of $4.3 \text{ MPa m}^{1/2}$ and an average grain size of 0.03 mm were used by Bergant et al. and they will also be used in the estimations that will be reported in sections 6.1 and 6.2. The fatigue endurance, $\Delta\sigma_{eR}$, used by Bergant was 254 MPa for the analysis of Solberg data and 315 MPa for the Andraeu's data. Details of their estimations can be found in reference [1].

3. THE CYCLIC R-CURVE FOR SHORT CRACK GROWTH

It has been accepted that the fatigue limit (or endurance) is not a critical stress for crack initiation but the one below which an initiated micro-crack cannot propagate. In other words, the plain fatigue limit, $\Delta\sigma_{eR}$, is in fact a threshold stress for micro-crack growth. This concept was clearly illustrated by Miller in reference [14] (see Figure 1).

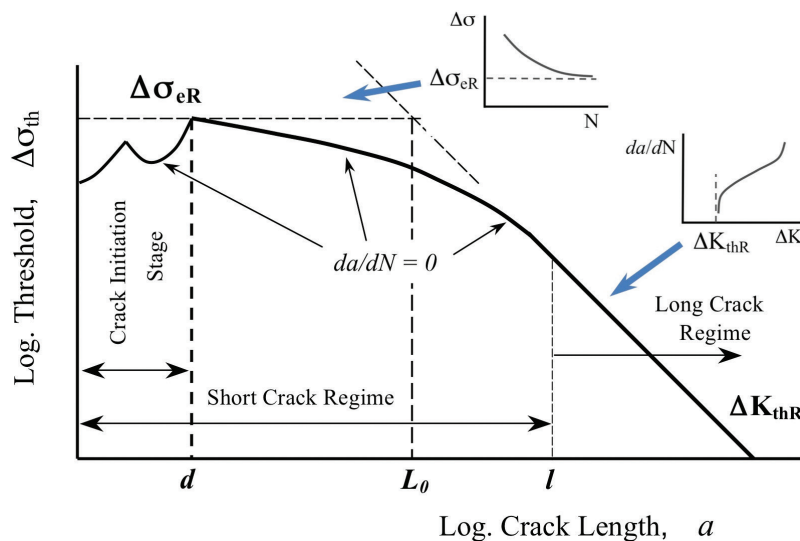


Figure 1: Kitagawa-Takahashi diagram showing the threshold for fatigue crack growth (cyclic resistance curve) in terms of stress range, after Ref [14].

Once the crack nucleates, it will grow up to the first grain boundary, or up to the strongest microstructural barrier and it is its arrest which defines the plain fatigue limit, $\Delta\sigma_{eR}$ (see Figure 1). This is a material-based limit (depending on the microstructural characteristic dimension, d) as Miller has pointed out [14]. Further early evidence can be found also along the deep analysis of Tanaka [15]. In previous works carried out by Chapetti and co-workers [16,17], the position and the effective resistance of microstructural barriers and their relation to the plain fatigue limit were analysed and modelled, and additional evidences that the strongest microstructural barrier defines the fatigue limit of plain and blunt-notched specimens in steels were obtained.

Figure 2 shows the cyclic resistance-curve concept in terms of the stress intensity factor range, where the total applied ΔK is compared with the threshold curve ΔK_{th} , which is equivalent to that shown in Figure 1 in terms of stress range, $\Delta\sigma_{th}$. In order for the crack to grow between these two limits (for instance, a_i and a_f), the applied ΔK has to exceed the ΔK_{th} threshold for every crack length (Figure 2a). The fatigue endurance of the configuration will be given by the applied nominal stress for which ΔK equals ΔK_{th} at any crack length in the integration interval (Figure 2b). In the last case, when stress gradient is presented, as in notched components, the maximum non-propagating crack length can be determined.

The schema shown in Figure 2(a) is used for fatigue life estimations in section 6.1. while the one shown in Figure 2(b) is used for the fatigue endurance estimations and defect assessment in section 6.2.

3.1. The IBESS approach

This approach is summarized in a special issue of the journal Engineering Fracture Mechanics [18] and in a textbook [19]. The IBESS approach (Integral method for fracture mechanics determination of the fatigue strength of weldments) is also based on the cyclic R-curve analysis and measures or estimates the threshold for crack growth ΔK_{th} as a function of the crack length by using the crack closure development concept [15,20–23], as follows:

$$\Delta K_{th} = \Delta K_{th,eff} + \Delta K_{th,op} \tag{1}$$

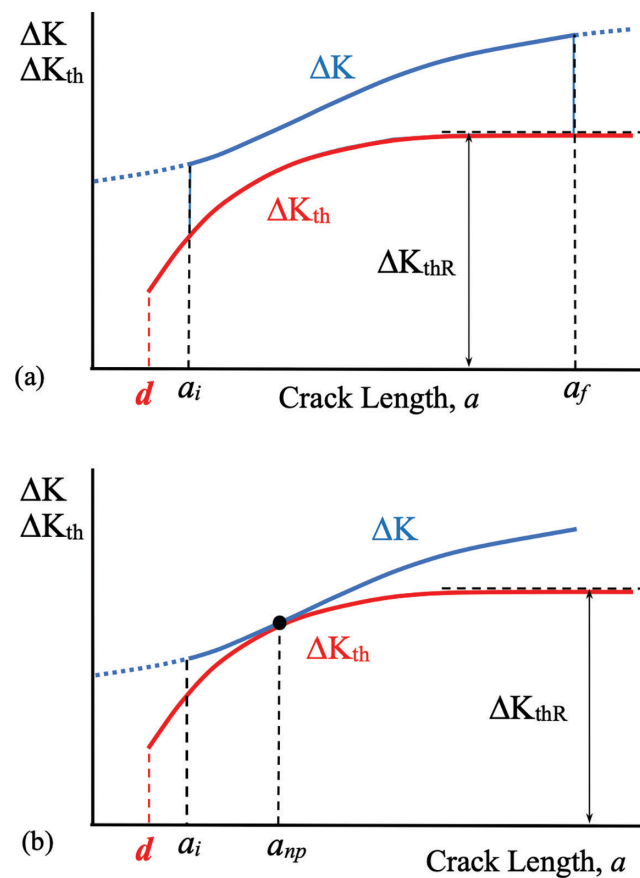


Figure 2: (a) Resistance curve concept. (b) Fatigue endurance of the configuration.

Once the cyclic R -curve (ΔK_{th} vs a) is measured or estimated, the fatigue crack propagation rate is determined by the following equation accounting for the crack closure and crack propagation threshold [1,18,19]:

$$\frac{da}{dN} = C[U\Delta K_p]^m \left[1 - \frac{\Delta K_{th}}{\Delta K_p} \right]^p \quad (2)$$

Where C , m and p are material constants, ΔK_p is the plasticity-corrected applied ΔK , and $U = \Delta K_{th,eff}/\Delta K$ is the crack closure factor of the short crack with $\Delta K_{th,eff}$ being the effective, i.e., crack closure corrected stress intensity factor range. The definition of U at the short crack stage is based on the correspondence with the cyclic R -curve [1,18,19]:

$$\frac{1-U_{SC}}{1-U_{LC}} = \frac{\Delta K_{th} - \Delta K_{th,eff}}{\Delta K_{thR} - \Delta K_{th,eff}} \quad (3)$$

The terms ΔK_{th} and ΔK_{thR} describe the short and long crack propagation thresholds and U_{SC} and U_{LC} are the short and long crack closure factor, respectively. The crack closure effect is then assumed to be absent for the initial crack and it is gradually built up until it approaches the crack size independent value U_{LC} for long cracks.

The highest-level analysis option within IBESS relies on the use of experimentally determined cyclic resistance curves (ΔK_{th} vs a) for the specific material and R -ratio. However, when this option is not available, a simple estimation method for its determination is proposed based on a modified El Haddad model, as follows [1,18,19]:

$$\Delta K_{th} = \Delta K_{thR} \sqrt{\frac{\Delta a + a^*}{\Delta a + a^* + a_0}} \quad (4)$$

The El Haddad model is modified by adding the correction parameter a^* chosen to fulfil the condition $\Delta K_{th} = \Delta K_{th,eff}$ for the strongest microstructural barrier associated to the endurance limit ($\Delta\sigma_{eR}$). a^* is estimated as follows [1,18,19]:

$$a^* = a_0 \frac{(\Delta K_{th,eff} / \Delta K_{thR})^2}{1 - (\Delta K_{th,eff} / \Delta K_{thR})^2} \quad (5)$$

Where a_0 is the intrinsic crack parameter proposed by El Haddad *et al.* to estimate the threshold curve (see Figure 3) [24]:

$$a_0 = \frac{1}{\pi} \left(\frac{\Delta K_{thR}}{Y\Delta\sigma_{eR}} \right)^2 \quad (6)$$

In this work the IBESS's approach is not analysed and the details for its application can be found in reference [1] where Bergant *et al.* made their analysis, or in references [18] and [19] where the model was introduced. However, the assumptions and hypotheses applied in the IBESS's proposal to estimate the threshold curve by using a modified El Haddad model (schematized in Figure 2), are analysed in Section 7.

The scheme in Figure 3 indicates that $\Delta K_{th,eff}$ is associated with the fatigue limit through $a_{0,eff}$, and that this parameter defines the strongest microstructural barrier. $a_{0,eff}$ is not constant for a given material but depends on the load ratio R , as a consequence of that $\Delta K_{th,eff}$ is constant but $\Delta\sigma_{eR}$ decreases with increasing R . This is a fundamental hypothesis of the crack closure-based models that has not been adequately demonstrated yet.

3.2. The Chapetti's model

An important hypothesis of the Chapetti's model is that the minimum intrinsic value of ΔK_{th} for crack propagation, associated with the fatigue limit (or endurance), can be estimated from the same fatigue limit and the average microstructural size d (e.g. grain size), as follows [25]:

$$\Delta K_{dR} = Y\Delta\sigma_{eR} \sqrt{\pi d} \quad (7)$$

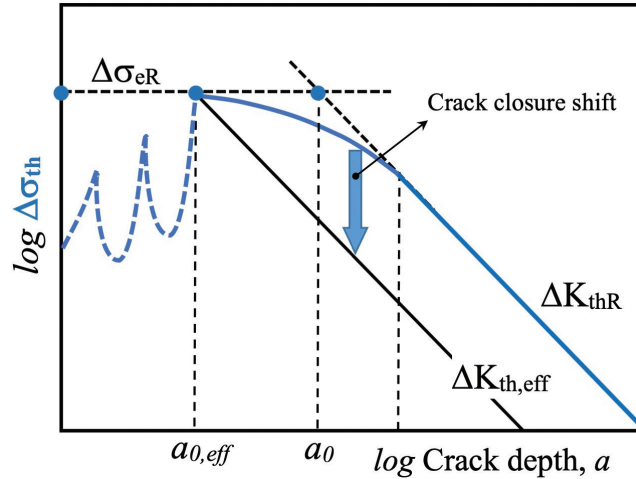


Figure 3: Crack closure model proposal for R-Curve estimation for short cracks. $\Delta\sigma_{th}-a$ [18,19].

where Y is the loading and geometric configuration correction factor. As in most cases microstructural short cracks nucleated at smooth surfaces are considered semi-circular [15,16,25,26], Y is taken conservatively as 0.65. This hypothesis derives from the concept that the fatigue limit is given by the ability of the strongest microstructural barrier (e.g. grain boundary) to arrest a micro-crack.

The ΔK_{dR} parameter, a microstructural threshold, represents the minimum driving force that can be apply to propagate a crack of size d . From this value, the threshold develops until reaching the maximum value defined by the long crack threshold, ΔK_{thR} . Figure 4 shows this concept in terms of the stress range (Kitagawa-Takahashi diagram).

The Chapetti’s model proposes that, in addition to ΔK_{dR} , the cracks growth threshold is also composed by an “extrinsic” component, a function of crack length and equal to $\Delta K_{th}-\Delta K_{dR}$. Once this component has fully developed, it reaches a maximum value (for long cracks), equal to $\Delta K_{thR}-\Delta K_{dR}$. Modelling the development of $\Delta K_{th}-\Delta K_{dR}$ which is a function of crack length with an exponential function, the following expression was proposed by Chapetti to estimate the threshold for short crack growth [25]:

$$\Delta K_{th} = Y\Delta\sigma_{th}\sqrt{\pi a} = \Delta K_{dR} + (\Delta K_{thR} - \Delta K_{dR})[1 - e^{-k(a-d)}] \tag{8}$$

where a is the crack length and k is a material constant given by the following expression [25]:

$$k = \frac{1}{4d} \frac{\Delta K_{dR}}{(\Delta K_{thR} - \Delta K_{dR})} \tag{9}$$

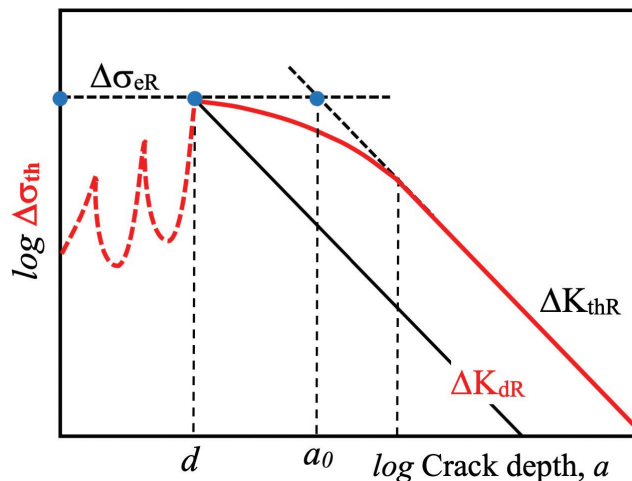


Figure 4: Chapetti model for R-Curve estimation for short cracks. $\Delta\sigma_{th}-a$.

Eqs. (8) and (9) are fully defined once $\Delta\sigma_{eR}$, ΔK_{thR} and d are known, all being parameters that can be easily obtained from common standardized fatigue tests and metallographic analysis. Further details of this model can be found in references [25] and [27].

Here it is important to mention that Bergant et al. indicate that in the Chapetti's model the resistance curve ΔK_{th} vs a is obtained by "fitting" the parameter k . The Eq. (9) is deduced from hypotheses associated with the proposed model and only the factor 4 comes from a fitting procedure on several sets of threshold data for short cracks made when it was proposed [25]. But when applying the model, the Eqs. (8) and (9) do not require any fitting procedure and provide pure estimation of the threshold curve.

Eq. (8) is also being used by different authors to estimate the resistance curve in models that consider as hypotheses that the minimum crack propagation threshold ΔK_{th} associated with the fatigue limit is given by the effective propagation threshold $\Delta K_{th,eff}$ with good results in analysis where the intrinsic length $a_{0,eff}$ associated with the fatigue limit has dimensions similar to the microstructural size d [1,5,6,26,28–30]. Something else will be said on this topic in section 7.

4. CRACK DRIVING FORCE

The driving force was calculated with the same procedure used by Bergman et al. [1], in order to analyse only the differences due to the procedures and hypotheses used to estimate the threshold resistance curve (ΔK_{th} vs a) and the fatigue lives. So the Murakami's *area* concept was applied for the estimation of the elastic crack driving forces ΔK of internal and surface defects [31–32]. The following expression for the total applied crack driving force ΔK was used [31–32]:

$$\Delta K = Y\Delta\sigma\sqrt{\pi\sqrt{area}} \quad (10)$$

with $Y = 0.5$ for internal defects and 0.65 for surface defects, $\Delta\sigma$ is the applied stress range and $area^{1/2}$ is the Murakami parameter proposed to correlate different types of defects, namely notches, indentations, cracks, and inclusions with the stress intensity factor range ΔK . In terms of an equivalent circular (internal) or semicircular (surface) crack length a , the following expression can be used [33,34]:

$$\Delta K = Y\Delta\sigma\sqrt{\pi a} \quad (11)$$

with $Y = 0,665$ for internal defects and $0,728$ for surface defects, respectively. Eq. (11) is used here for result reports (ΔK as a function of crack length, a).

In the IBESS approach, ΔK has still to be corrected to include plasticity effects, correction that was made according to BS 7910 recommendation [35] in the analysed paper (Bergant et al. [1]). The applied driving force is given by the applied elastic ΔK in Chapetti model and by the plasticity-corrected ΔK_p in IBESS model (see Eq. 2). The difference in the way of estimating the driving force leads to the assumption that $\Delta K_p(a) > \Delta K(a)$ since the plasticity effects will always increase the crack driving force, and that crack propagation will be then faster in the IBESS's approach (considering similar R -curves), leading to more conservative fatigue life assessments. However, as it was pointed out in reference [1] it should be noted that the threshold R -curves are defined differently in both approaches and that the effective crack driving force for crack propagation in Chapetti's and the IBESS models follows different expressions. These differences will be analysed in the following sections, together with the description of the application procedure of the Chapetti's model carried out in the present work.

5. FATIGUE CRACK PROPAGATION RATE ESTIMATION

Bergant et al. indicated that the Chapetti's approach uses the expression proposed by Klesnil and Lukas to estimate the crack propagation rate, da/dN , as a function of the driving force ΔK and the crack threshold ΔK_{th} , both as a function of the crack length a [36]:

$$\frac{da}{dN} = C^*(\Delta K^{m^*} - \Delta K_{th}^{m^*}) \quad (12)$$

Were C^* and m^* are the constants dependent on the material, the environment and the load-ratio R . However, nowadays this author prefers the following formula for crack propagation rate [37]:

$$\frac{da}{dN} = C(\Delta K - \Delta K_{th})^m \quad (13)$$

The preference of the expression (13) over (12) is due to the fact that it predicts higher propagation rates when used to analyse short cracks (see reference [27] for details). So, expression (13) is used in this work for estimations. However, more complex expressions can be used, and there are no limitations to use the one deemed appropriate.

Eqs. (12) and (13) contemplate the concept of the resistance curve, and include the short crack regime if ΔK_{th} accounts for the threshold development (ΔK_{th} vs a). $C = 6,25 \times 10^{-10}$ mm/cycle and $m = 3,94$ were reported in [1] for Eq. (12), and they were estimated here as $C = 1,15 \times 10^{-7}$ mm/cycle and $m = 2,2$ for Eq. (13).

The integration of Eq. (13) is performed between the initial crack length, a_i , given by the defect size or by the microstructural size d (end of the initiation stage), and a final crack length, a_f , that would be related to the configuration that defines the end of the mechanical life of the component (failure, fracture, etc). In order for the crack to grow between these two limits, the applied ΔK has to exceed the ΔK_{th} threshold at any crack length. Figure 5(a) shows schematically the R-curve concept for this configuration.

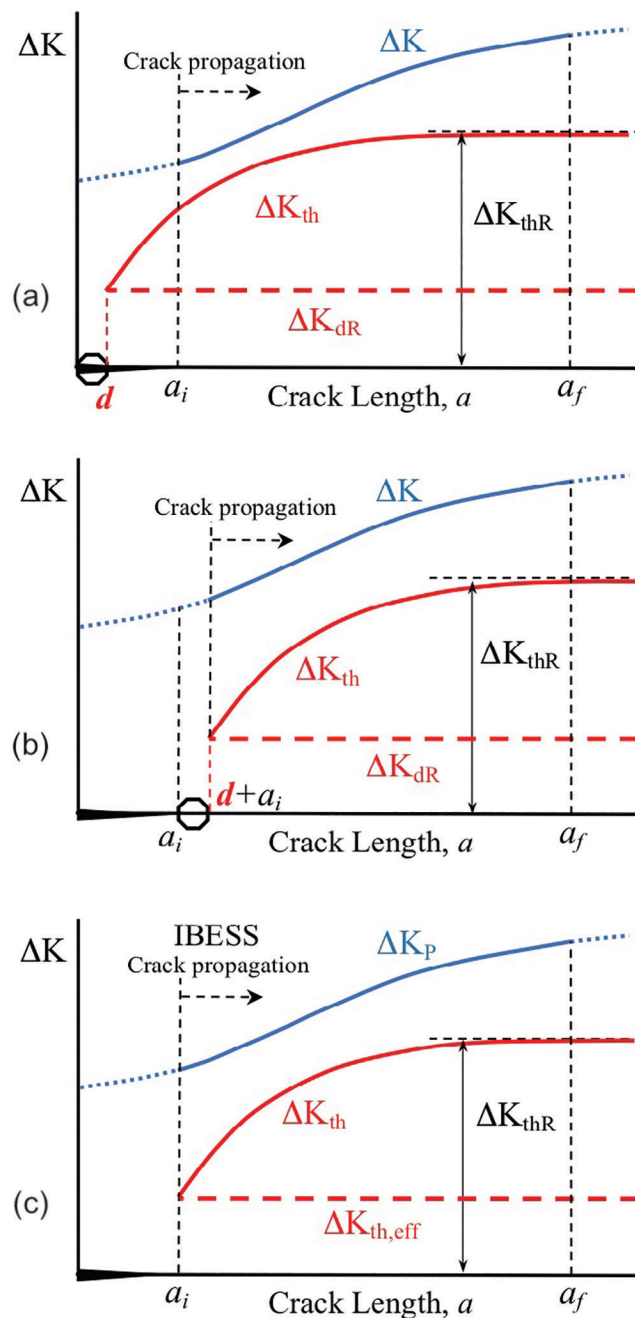


Figura 5: Cyclic R-curve concept and fatigue life configuration for estimations. (a) Present analysis, used also by Bergant [1]. (b) Alternative configuration used by Bergant when applying the Chapetti's model [1]. (c) IBESS criteria applied by Bergant [1].

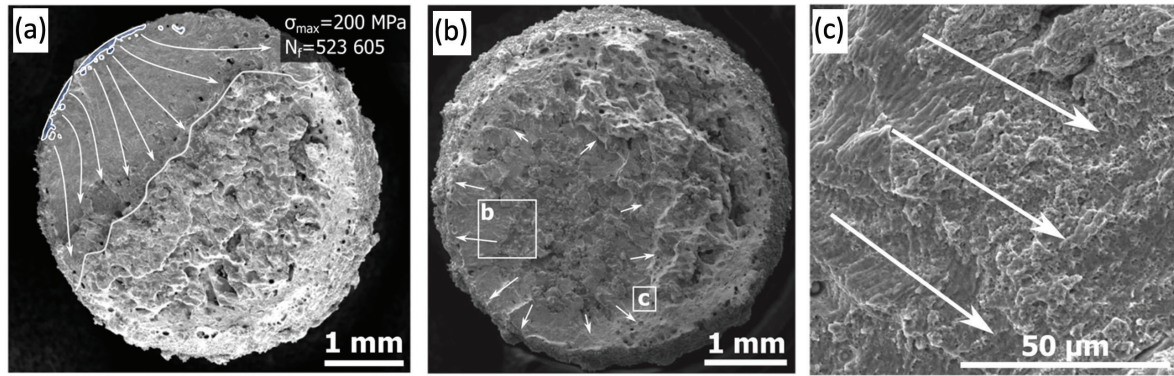


Figure 6: Scanning electron microscopy (SEM) of fracture surfaces. a) fracture from a surface defect. b) whole fracture surface of specimen failing from internal defect, c) transition from striations to ductile failure. The arrows are indicating the direction of crack propagation (taken from Solberg et al. [11]).

Figs. 5 (b) and (c) reproduce two other criteria analysed by Bergant et al. Figure 5(b) corresponds to another version of the Chapetti's approach for the starting point of the cyclic R -curve at the abscissa ($a_i + d$). To consider this variant Bergant et al. refer to publications where the Chapetti's approach is used to analyse relatively blunt notches. The present author think that it does not correspond to this case and that to apply the configurations of Figure 5(b) it is necessary to consider the relative value of the extension of the short crack regime with respect to the size of the notch (or defect). This topic will be analysed by the present author in a future publication. In this work, only the configuration of Figure 5(a) will be applied. It is necessary to comment here that if the configuration indicated in Figure 5 (b) is used to apply the Chapetti's model in the present case, the fatigue life estimations should give lower values (and therefore should be more conservative) than those estimated by the configuration of Figure 5(a), and the difference would depend of the initial defect size.

Besides, Bergant et al. used the configuration shown in Figure 5(c) to applied the IBESS's approach, so that the defect dimension is equal to the initial crack length for the crack growth resistance curve. That is to say, ΔK_{th} is equal to $\Delta K_{th,eff}$ for $a = a_i$.

Furthermore, it is necessary to consider the photographs of the fracture surface reported by Solberg et al. [11] that allow an analysis of the propagation rate data (values of C and m) and the upper limit for the integration of the expressions of da/dN used by Bergant et al. [1] ($K_{max} = 16.7 \text{ MPa m}^{1/2}$).

Figure 6 reproduces some fractographs published by Solberg et al. for a fracture initiated from surface and internal defects [11]. Figure 6(c) corresponds to a fracture surface initiated by an internal defect that shows striations associated to the last part of the fatigue crack growth stage, with spacings between 1 micro-meters and 2.5 micro-meters corresponding to crack growth rates between 10^{-3} and 2.5×10^{-3} mm/cycle. From the crack propagation rates properties reported and used for the estimations by Bergant et al. those growth rates correspond to applied ΔK of more than $40 \text{ MPa m}^{1/2}$, more than twice the maximum K value considered by those authors for the estimations. In addition, the photographs in Figure 6(a) and (b) show that the defects do not propagate more than 1–1.2 mm before fracturing the samples. Therefore, for the estimations in the present work, a maximum final crack length of 1.2 mm is additionally considered as another limit of integration of the Eq. (13), and a growth rate of an order of magnitude greater than those reported and used by Bergant *et al.* is here used ($C = 1,15 \times 10^{-6}$ mm/cycle).

6. RESULTS AND DISCUSSIONS

6.1. Estimation of S-N curves for fracture from material defects

Figure 7 shows all experimental data published by Solberg et al. [11] (full black round symbols for fracture from superficial defects, and black hollow rounds symbols for fracture from internal defects), the estimations obtained by Bergant et al. [1] applying the IBESS's approach and the Chapetti's model (red triangular symbols), and the estimations carried out in the present work (blue and green symbols and lines). Only the estimations obtained by Bergant et al. applying the Chapetti's model and the configuration illustrated in Figure 5(a) is reported here for the analysis (hollow red triangle symbols). Here it is important to note that for this configuration the estimations in all cases overestimated the experimental results. The estimations made by Bergant et al. for the configuration shown in Figure 5(b) is not analysed here because this author considers that they should yield

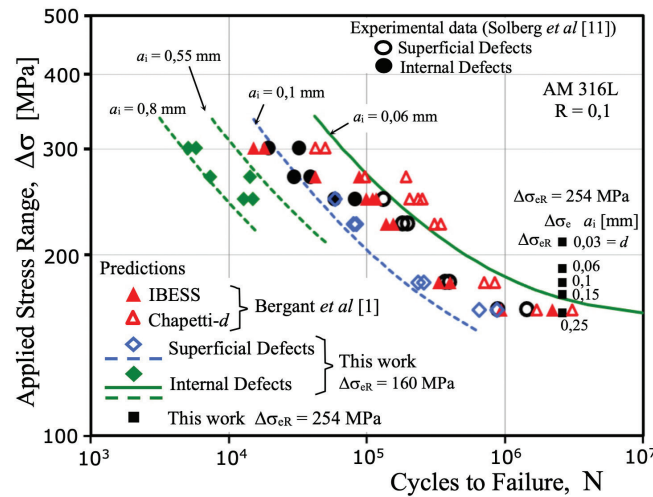


Figure 7: $\Delta\sigma$ -N data and curves for AM 316L. Experimental data from Solberg et al. [11] and predictions reported by Bergant et al. [1] and carried out on the present work.

clearly conservative results, particularly for fractures generated from defects up to 0.55mm. More details on the experimental data reported by Solberg and used by Bergant can be found in references [11] and [1], respectively.

An important issue to highlight is that the fatigue endurance ($\Delta\sigma_{er}$), reported in the work by Bergant for the estimations, is 254 MPa. This value is much higher than the fatigue endurance associated with the experimental data published by Solberg, which is around 160–165 MPa. In Figure 7 the solid black square symbols indicate the fatigue endurance estimated in the present work for $\Delta\sigma_{er} = 254$ MPa and different initial crack lengths: $a_i = d$ (0,03mm), 0,06, 0,1, 0,15 and 0,25 mm. The estimated fatigue endurance of about 160 MPa requires an initial defect size equal to $a_i = 0,25$ mm, much larger than the sizes of defect observed by Solberg in specimens tested at levels close to the fatigue endurance (0,06 mm). Besides, in the case of fracture from surface defects, the maximum defect size observed by Solberg was 0,14 mm. It is obvious that the results obtained by Bergant et al. when applying the Chapetti’s model would overestimate the experimental results, as can be observed in Figure 7 (hollow red triangle symbols).

Here it is necessary to make some remarks. Bergant et al. estimated the plain fatigue limit of the material tested by Solberg [11] from the tensile strength (437 MPa), applying the IBESS’s suggestion for the correlation between the fatigue limit and the ultimate tensile strength for conventional austenitic stainless steels, $\Delta\sigma_{er} (R = -1) = 0,8 \sigma_U$, and doing the R correction to the one corresponding to the load ratio $R = 0,1$ through the Goodman’s equation, getting $\Delta\sigma_{er} = 254$ MPa. This procedure contrasts, in terms of reliability, with the detailed analysis carried out to quantify the total force applied to the defect, ΔK_p , which means that the resistance curve ΔK_{th} - a estimation contains comparatively much higher uncertainties. The defect size associated to the observed fatigue endurance of about 162 MPa was 0,06 mm (see Figure 7), twice the grain size d that is equal to 0,03 mm. This shows that the intrinsic fatigue endurance $\Delta\sigma_{er}$ of the material without defects would not be so different (and it should be equal to or smaller, not greater), so the value of 254 MPa appears to be an overestimation. From all the actual reported experiences with additive manufacturing materials, it is clear that all the variables necessary to make the analysed estimations must be measured appropriately for the material under study. Otherwise, the estimations will be somewhat unreliable.

Therefore, and taking into account the previous analysis, for the estimations made in the present work a fatigue limit of 160 MPa is used, assuming that it would represent the endurance of the material without defects or defects with sizes up to a value similar to the grain size d (0.03 mm). Figure 7 shows estimations for the defect sizes reported by Solberg et al. for different tests with their respective levels of applied nominal stresses (symbols), and for certain flaw sizes and for the entire stress range (S-N curves, lines). It can be observed that acceptable and conservative results were obtained for all estimations, that are in much better agreement with the data corresponding to fractures from surface defects and at stress levels close to the fatigue endurance, region in which linear-elastic fracture mechanical models have greater applicability.

Estimated $\Delta\sigma$ -N curves for fracture initiated at internal defects with equivalent $a_i = 0,06 (= 2d)$, 0,55 and 0,8 mm are shown in Figure 7, and are also acceptable, although very conservative. This may be a consequence of the simplifying hypotheses regarding defects (of large size, especially regarding the integration interval in terms of crack lengths), and of the assumed crack propagation rate constants. The estimations are almost an

order of magnitude smaller than the fatigue lives experimentally observed, but beyond the aforementioned simplifications that make the estimates very conservative for this case (but safe), they clearly show that the procedure can account for the influence of the initial crack length given by the defect size (a statistical analysis can be added if necessary). The analysis shows that estimation procedures must be applied ensuring that each parameter involved is conservatively measured or estimated in order to avoid dangerous overestimations. The estimations obtained in the present work are in agreement with those concepts and clearly contradict the overestimations (unsafe) obtained by Bergant et al. using the same model for the threshold curve (Chapetti).

6.2. Fatigue endurance estimation and defect assessment

Figure 8 shows a K-T diagram with the experimental results published by Andreau et al. [12], the estimations published by Bergant et al. (with both the IBESS's approach and the Chapetti's model, blue and green lines, respectively), and the estimations carried out in the present work by using the Chapetti's model to estimate the threshold curve $\Delta\sigma_{th}$ vs a (red lines). For this analysis the following data were used [1]: fatigue endurance of the material $\Delta\sigma_{er} = 315$ MPa, long crack propagation threshold $\Delta K_{thr} = 4.3$ MPa $m^{1/2}$, and an average grain size $d = 0.03$ mm.

Figure 8 shows several differences on the estimations. Bergant obtained stress range threshold values associated to the experimental results somehow greater than the fatigue endurance of the material. This would be the case if the estimations were associated with a given crack propagation rate greater than that corresponding to the fatigue endurance (near zero, or very low). In fact, in reference [1] it is reported that the propagation threshold estimated with the IBESS method would be given by the continuous blue curve shown in Figure 8. The dashed lines would then be indicating a given propagation rate of cracks of similar sizes to the defects found by Andreau in the tested and fractured specimens. However, Chapetti proposed his model to estimate the threshold curve for the analysed material, that is, $\Delta\sigma_{th}$ (or ΔK_{th}) as a function of the crack length a , above which a crack could propagate, regardless of the propagation rate that the crack has. Obviously, for nominal stresses that make the applied $\Delta\sigma$ greater than the $\Delta\sigma_{th}$, the cracks would propagate at rates given by Eq. (13) or any other that is being used for the estimation. Therefore, to compare the performance of the threshold curve prediction models, the continuous red and blue curves should be compared, estimated by the models proposed by IBESS and Chapetti, respectively. Doing so, it can be observed that the Chapetti model can explain all fracture data except one. The red dashed line was added in order to show the influence of the parameter Y in the estimation of the threshold curve, changing $Y = 0,65$ used by Chapetti for $Y = 0,728$ used by Bergant. Besides, it is clear that in terms of the threshold stress range both models predict very different curves, with very different associated short crack ranges. In the case of the prediction of the Chapetti model, the threshold is fully developed for crack length on the order of 0,5 mm, while for the Bergant estimation using IBESS the threshold has barely been developed for a crack length of 1 mm.

These differences are again observed in the results recently published by Pourheidar et al., who measured and analysed the cyclic R -curve for a EA4T steel [38]. They also presented different testing procedures employed in the experimental determination of the cyclic R -Curve, especially focusing on the comparison with

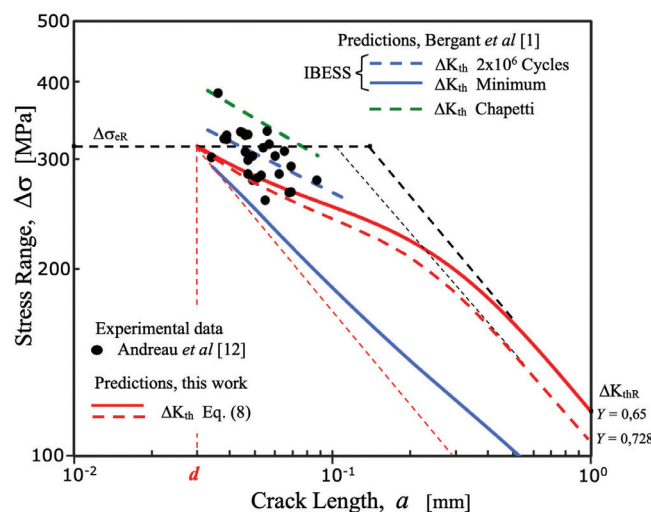


Figure 8: K-T diagram, threshold stress range as a function of crack length. Experimental data by Andreau et al. [12], estimations carried out by Bergant et al. [1], and present estimations.

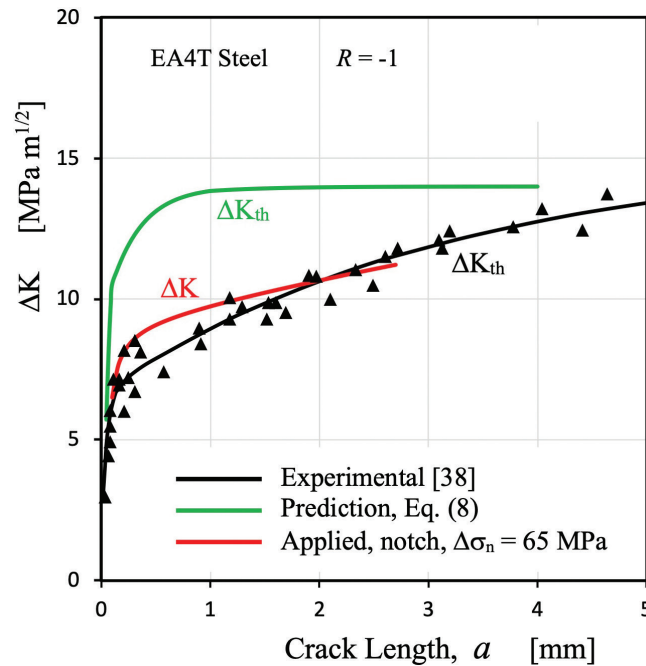


Figure 9: Thresholds (experimental measured [38], and estimated with Eq. (8)) for EA4T steel.

long fatigue crack propagation thresholds obtained by means of the compression pre-cracking load reduction procedure. Figure 9 presents the propagation threshold measured experimentally in [38] for $R = -1$, as a function of the crack length and in terms of the range of the stress intensity factor (black symbols and black line). The green line corresponds to the propagation threshold estimated with expression (8) (Chapetti's model), and would be similar to that estimated by the El Haddad model [24], or the Murakami model [31].

It can be seen that in the case of predictions the ΔK_{th} threshold develops completely in the first millimetre of crack propagation, while for the experimentally measured threshold it is still developing for depths of 3 mm. Analysing the differences, we can infer that a component with a 1 mm deep crack would have an associated fatigue limit of 143 MPa for the experimentally measured threshold, while for the estimated one it would be 222 MPa, 55% higher. Figure 9 also shows the applied ΔK for the case of a crack propagating from a superficial semi-elliptical notch 5 mm deep and 2 mm wide (red line), with a nominal stress range $\Delta\sigma_n = 65$ MPa (estimated from [39]). The crack could propagate and eventually be arrested at a depth of about 2 mm, but the thresholds estimated with the available predictive models do not allow predicting a possible crack propagation. It is very clear that these differences raise many questions that must be answered. There will thus be the need to generate important experimental evidence in order to clarify the sources of discrepancies.

The next section completes the analysis by making general observations associated with the threshold prediction models, their hypotheses, their combinations and their relationship to the K-T diagram.

7. KITAGAWA-TAKAHASHI DIAGRAM. THRESHOLD CURVE PREDICTION MODELS AND HYPOTHESES.

An important issue to note is that the intrinsic fatigue limit, $\Delta\sigma_{GR}$, used in the models (or at least in the models of Chapetti, El Haddad and those that use the concept of crack closure), should be the one that agrees with the hypothesis that the fatigue limit is given by the strength of the strongest microstructural barrier. This concept, explained very clearly by Miller in references [14] (see Figure 1), defines a minimum microstructural threshold for the propagation of cracks initiated by fatigue in polished specimens or components. Figure 4 shows the K-T diagram with the threshold defined by Chapetti with this hypothesis included. In this model, this minimum value is equal to ΔK_{GR} given by Eq. (7). This has a consequence, that the fatigue endurance to be used must represent the resistance to crack initiation of the material without defects greater than d , a value that defines the average distance to the strongest microstructural barrier from the surface of the material. This hypothesis is included also in the modified El Haddad model used by Bergant et al. to estimate the cyclic R -curve (Eq. 4, see Figure3). As in the case of the models that use the concept of crack closure, the Eq. (1) uses the hypothesis that the microstructural threshold associated with the fatigue limit of the material is given

by the effective threshold of long cracks. In this case, the position of the strongest barrier is given by the parameter $a_{0,eff}$ defined as (see Figure 3):

$$a_{0,eff} = \frac{1}{\pi} \left(\frac{\Delta K_{th,eff}}{Y \Delta \sigma_{eR}} \right)^2 \quad (14)$$

The value of $a_{0,eff}$ is not constant and depends on the load ratio R . As R increases, and taking into account that $\Delta K_{th,eff}$ does not depend on R in a first approximation, the fatigue limit decreases and therefore $a_{0,eff}$ increases. This has not been demonstrated experimentally and the experience of this author with the analysis of non-propagating cracks associated with the plain fatigue limit is that the tendency is to decrease or disappear, not to increase, as R increases. For this hypothesis to be validated, detailed experimental work is necessary. In addition, this work must be carried out analysing naturally initiated cracks, not using artificial defects, because the fatigue limit is given by the weakest microstructural configurations in microstructural entities favourably oriented to induce surface strain concentrations. Figure 10 reproduces the illustration proposed by Abdel-Raouf, Topper and Plumtree to explain the inherent surface strain concentration [40,41].

Abdel-Raouf et al. explained that the material at a free surface will deform more easily than in the interior which is surrounded and supported by other grains (the constrain increases with depth). Besides, and because the free surface of polycrystalline alloys represents a section through a large number of randomly oriented grains whose operating slip system will have different orientations with respect to the loading axis, a redistribution strain process takes place. They argued that the strain in each surface layer is accommodated by the lack of restraint and this local strain is proportional to the corresponding orientation. Favourably orientated grains experience the largest amount of surface deformation and the greatest amount of localized slip occurs, representing a

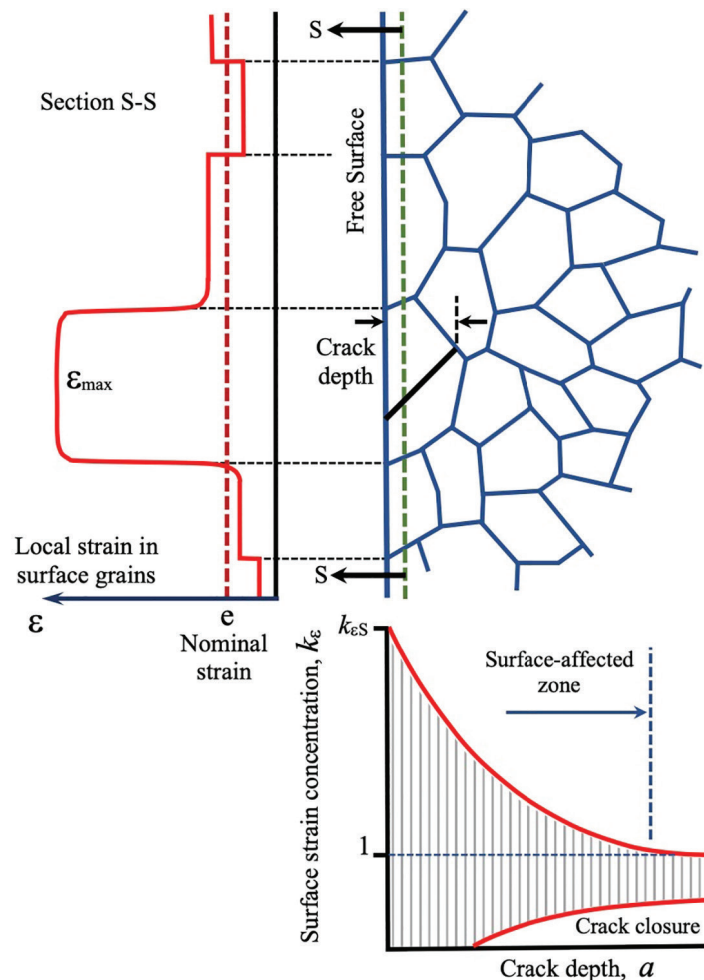


Figure 10: Surface strain redistribution. After Abdel-Raouf et al [40,41].

preferred site for crack initiation. The correspondingly large local strain decreases with depth, approaching the nominal strain range. This decay is due to the increasing constraint and strain compatibility requirements. They also argued that if the rate of decay is controlled by the grain size d , then the larger the grain, the deeper the local resolved shear strain (larger deformation) and also less surface area per unit volume of contact between this favourably oriented grain and its neighbouring grains (hence less constraint). This surface effect, added to the transition associated with the change in crack propagation mode (Mode II to Mode I), makes the extrapolation of the effective threshold for long cracks, $\Delta K_{th,eff}$, inadequate, since it cannot contemplate or quantify the previously described effects. An illustration proposed by Abdel-Raouf et al. to explain this matter is also reproduced in Figure 9. For the case of small cracks, of sizes that do not exceed 4 or 5 microstructural entities, the propagation threshold cannot be estimated by quantifying only the crack closure effect.

Those phenomena were considered by Chapetti when proposing his model. The minimum threshold ΔK_{dR} (see expression 7) is defined by the experimentally measured plain fatigue limit, $\Delta\sigma_{eR}$, which implicitly quantifies all the phenomena mentioned above.

Throughout his work, Bergant et al. carried out two analyses on this topic that to a certain extent contradict each other or are not fully compatible. At first, they argued that “*the size of the microstructurally short crack associated with the fatigue limit usually is not just one but a number of grain sizes. A rough number for this is three [31], but this varies depending on the material*”, referencing Murakami and his experimental work on the influence of defects. They indicated that the reason is the mechanism of crack arrest at grain boundaries, which is associated with an increased energy needed to overcome the barrier when the neighbouring grains significantly differ in crystal orientation. Here it is clear that they mean that the strongest microstructural barrier is not the first grain boundary, but, for example, the third. Studies carried out by the author of the present work [16,17,42] indicate that the resistance of the second grain boundary, or the third, and so on, discreetly define the resistance curve of the material as a function of the crack length, which in terms of ΔK shows a resistance increasing, but in terms of stresses it shows a resistance decreasing. In this way, in the K-T diagram, the strongest barrier that is finally associated with the fatigue limit in the first one. It is possible that other barriers may appear located at smaller distances (given for example by second phases), but in general the position of the strongest barrier associated with the fatigue limit is given by the average size of some of the microstructural entities. Bergant et al. seems to agree with these concepts a few paragraphs later, when describing the K-T diagram. Taking into account that the highest-level analysis option within IBESS relies on the use of experimentally determined cyclic R-curves (ΔK_{th} vs a), all hypothesis of the different alternative options should be clarified and demonstrated.

Besides, Bergant et al. analysed the configurations reported by Solberg and Adreau by applying the Cyclic R-curve (ΔK_{th} vs a) with the criteria illustrated in Figure 5(c). If that criteria is used the minimum threshold for crack growth is given by $\Delta K_{th,eff}$ for the initial crack length that it is given by the size of the defect that nucleated the crack that produces the fatigue fracture. The differences in results obtained by applying criteria of Figure 5 (a) and (c) will increase as the defect size increases. This is a strong assumption that should be clearly demonstrated, because its validity depends strongly on the defect size, nature, and shape. The author think that the crack closure effect starts to develop when the cracks nucleated from the defects, but the development rate will depend of the defect size, that it is say, it will depend of the total equivalent initial crack length involve in the configuration (defect plus crack). Once the nucleated crack start to growth, the stress field at the crack tip is defined by the full configuration (nominal applied stress and the total crack length).

Finally, it is important to discuss here some issues involved in the application of the fracture mechanics models to estimate the threshold curve when the criteria illustrate by Figure 5(a) is used. Most of the recently published works that analyse the influence of inherent defects on the fatigue endurance (for instance in additive manufactured alloys), estimate the thresholds curve by using the models of El Haddad [24], Chapetti [25], those based on the crack closure development (mainly that proposed by McEvily et al. [21–23]), or other modifications or combinations of those. In most applications they were used and/or mixed with a certain degree of care (and in many cases very little) of the fundamental bases of their proposals.

Because the crack closure models need non-trivial experimental tasks El Haddad and Chapetti’s models are sometimes preferred for estimations [1–10,28–30,43,44], because they need only to measure ΔK_{thR} and $\Delta\sigma_{eR}$ (plus d for the last case). If it is necessary to deal with the minimum ΔK_{th} for fatigue crack propagation, the Chapetti’s model is preferred which allows estimating it with the parameter ΔK_{dR} .

Different applications of the Chapetti’s model can be found in the literature and many of them mistakenly confused the parameter ($\Delta K_{th} - \Delta K_{dR}$) with the crack closure component ($\Delta K_{th} - \Delta K_{th,eff}$), and therefore with the model proposed by McEvily, so that Eq. (8) becomes (see for instance references [28], [29] or [30]):

$$\Delta K_{th} = \Delta K_{th,eff} + (\Delta K_{thR} - \Delta K_{th,eff})[1 - e^{-k(a-d)}] \quad (15)$$

Even with the recent clarification made in reference [27], more researchers continue making erroneous analysis and applications of the model (see for instance [3] and [30]). The other important difference between the models is that the parameter k used to describe the development of the threshold ΔK_{th} should be obtained by fitting experimental data of short crack thresholds for the closure models. Instead, in the Chapetti model k is estimated with ΔK_{thR} , $\Delta \sigma_{eR}$, d and Eq. (9). Besides, Eq. (9) can be applied for any alloy and makes the model a real estimation tool. After this clearly wrong assumption, the parameter k given by Eq. (9) is in most cases used to estimate the development of the crack closure component ($\Delta K_{th} - \Delta K_{th,eff}$), by replacing ΔK_{dR} by $\Delta K_{th,eff}$ as follows:

$$k = \frac{1}{4d} \frac{\Delta K_{th,eff}}{(\Delta K_{thR} - \Delta K_{th,eff})} \quad (16)$$

When the defects size below which it become non-detrimental for fatigue strength is estimated by using Eq (15), the effective threshold for long crack $\Delta K_{th,eff}$ is commonly used, together with the plain fatigue limit (intrinsic crack length $a_{0,eff}$, expression 14, see Figure 3). In some cases it is even expressly stated that the minimum threshold for crack propagation cannot be less than that given by the $\Delta K_{th,eff}$. There is a lot of evidence in the literature that shows values of ΔK_{th} associated with the fatigue limit lower than $\Delta K_{th,eff}$.

Modifications of existing prediction models are sometimes proposed that neglect the assumptions used by the models being modified, without considering the consequences on the estimations and their certainty. In a recent publication, Leonetti *et al.* [30] added a modification to the Eq. (9) to calculate the parameter k applying the Murakami model and other assumptions. Finally, they make comparisons of the estimations of the IBESS approach (modified El Haddad, Eq. 4), Chapetti's model (Eq. 8), FITNET proposal [45] and its new proposal [30], in which they clearly take the experimental data from reference [25] and make $\Delta K_{th,eff} = \Delta K_{dR}$ (last one estimated by using Eq. 7). Obviously in this case $\Delta K_{th,eff}$ will not be constant for a given material but will depend on the load ratio R , contradicting the basic concept of the effective threshold for crack growth (independent of R).

It is clear from the analyses that care must be taken with the combinations of models, hypotheses, and physical meaning of the variables used, and that additional work is needed to clarify several related issues. Further analysis on these topics can be found in reference [46].

Finally, it is necessary to point out that it is necessary to analyse the configuration illustrated in Figure 5(b) used by Bergant *et al.* to analyse the Solberg [11] and Andreau [12] data, and by Chapetti to analyse notched configurations [47–49] (relatively blunt). This topic requires a more detailed analysis because it involves transitions related with the size of the notch, and even with respect to the microstructural size. This topic becomes important for defects considered as notches (in the case of volumetric defects), and will be dealt with in a future publication.

8. CONCLUDING REMARKS

Fracture mechanics-based models allow estimating the behaviour of short cracks and make possible the estimations of fatigue lives and fatigue limits (or endurance) of components with small cracks or crack-like defects generated during manufacturing. For these cases, the elimination or significant reduction of the crack initiation stage allows analysing its resistance to fatigue by quantifying only the crack propagation stage. In this way it is possible to use fracture mechanics models to estimated $\Delta \sigma$ - N curves (fatigue lives) for design and optimization stages of mechanical components.

Discrepancies observed and discussed in this work show the importance of having measured data for the analysed material and the errors that can be made when using measured values for others, especially in materials produced with additive manufacturing in which the properties depend on many parameters for the same powder.

Particularly, the estimations reported here and the comparative analyses with respect to the ones reported by Bergant *et al.* show that it is possible to obtain large discrepancies in the results if the hypotheses, limitations, and appropriate conservative procedures are not clearly defined for choosing and/or deriving the data or models to be used.

The analyses made also showed that there are still several issues that should be clarified, mainly related with the hypotheses of the fracture mechanics available models, their combinations and their limitations that should be clearly demonstrated, as well as the consequence of their combinations. Besides, it is common to see contradictions between the hypotheses of the models and those added when applying them. For instance, the estimation of the minimum threshold for crack growth associated to the plain fatigue limit will always have an associated characteristic crack length, which has to be related to the microstructural configuration that defines it. All assumed hypotheses or simplifications should consider this concept.

Finally, this author thinks that when applying the fracture mechanics models special attention is necessary when comparing intrinsic strengths of the analysed material and that of material-defect combinations, particularly when the defects used in the analysis are artificial and/or are relatively large comparing with the microstructural dimension.

9. ACKNOWLEDGMENTS

Author wishes to express his gratitude to the funding provided by Agencia Nacional de Promoción Científica y Tecnológica, Argentina (PICT 2017 Nro. 0982).

10. REFERENCES

- [1] BERGANT, M., WERNER, T., MADIA, M., *et al.*, “Short crack propagation analysis and fatigue strength assessment of additively manufactured materials: An application to AISI 316L”, *International Journal of Fatigue*, v. 151, 106396, 2021.
- [2] ZERBST, U., VORMWALD, M., PIPPAN, R., *et al.*, “About the fatigue crack propagation threshold of metals as a design criterion – a review”, *Engineering Fracture Mechanics*, v. 153, pp. 190–243, 2016.
- [3] HU, Y.N., WU, S.C., WITHERS, P.J., *et al.*, “The effect of manufacturing defects on the fatigue life of selective laser melted Ti-6Al-4V structures”, *Materials and Design*, v. 192, 108708, 2020.
- [4] SCHÖNBAUER, B.M., YANASE, K., ENDO, M., “VHCF properties and fatigue limit prediction of precipitation hardened 17-4PH stainless steel”, *International Journal of Fatigue*, v. 88, pp. 205–216, 2016.
- [5] SCHÖNBAUER, B.M., YANASE, K., ENDO, M., “The influence of various types of small defects on the fatigue limit of precipitation-hardened 17-4PH stainless steel”, *Theoretical and Applied Fracture Mechanics*, v. 87, pp. 35–49, 2017.
- [6] SCHÖNBAUER, B.M., MAYER, H., “Effect of small defects on the fatigue strength of martensitic stainless steels”, *International Journal of Fatigue*, v. 127, pp. 362–375, 2019.
- [7] KEVINSANNY, S.O., TAKAKUWA, O., OGAWA, Y., *et al.*, “Effect of defects on the fatigue limit of Ni-based superalloy 718 with different grain sizes”. *Fatigue and Fracture of Engineering Materials and Structures*, v. 42, n. 5, pp. 1203–1213, 2019.
- [8] HU, Y.H., WU, S.C., WU, Z.K., *et al.*, “A new approach to correlate the defect population with the fatigue life of selective laser melted Ti-6Al-4V alloy”, *International Journal of Fatigue*, v. 136, 105584, 2020.
- [9] MOLAEI, R., FATEMI, A., “Fatigue design with additive manufactured metals - Issues to consider and perspective for future research”, *Procedia Engineering*, v. 213, p. 5–16, 2018.
- [10] MOLINA, C., ARAUJO, A., BELL, K., *et al.*, “Fatigue life of laser additive manufacturing repaired steel component”, *Engineering Fracture Mechanics*, v. 241, 107417, 2021.
- [11] SOLBERG, K., GUAN, S., RAZAVI, S.M.J., *et al.*, “Fatigue of additively manufactured 316L stainless Steel: the influence of porosity and surface roughness”, *Fatigue and Fracture of Engineering Materials and Structures*, v. 42, pp. 2043–2052, 2019.
- [12] ANDREAU, O., PESSARD, E., KOUTIRI, I., *et al.*, “A competition between the contour and hatching zones on the high cycle fatigue behaviour of a 316L stainless steel: analyzed using X-ray computed tomography”, *Material Science and Engineering A*, v. 757, pp. 146–159, 2019.
- [13] RIEMER, A., LEUDERS, S., THÖNE, M., *et al.*, “On the fatigue crack growth behavior in 316L stainless steel manufactured by selective laser melting”, *Engineering Fracture Mechanics*, v. 120, pp. 15–25, 2014.
- [14] MILLER, K.J., “The two thresholds of fatigue behaviour”, *Fatigue and Fracture of Engineering Materials and Structures*, v. 16, n. 9, pp. 931–939, 1993.
- [15] TANAKA, K., NAKAI, Y., YAMASHITA, M., “Fatigue growth threshold of small cracks”, *International Journal of Fracture*, v. 17, n. 5, pp. 519–533, 1981.
- [16] CHAPETTI, M.D., TAGAWA, T., MIYATA, T., “Fatigue notch sensitivity of steel blunt notched specimens”, *Fatigue and Fracture of Engineering Materials and Structures*, v. 25, n. 7, pp. 629–634, 2002.
- [17] CHAPETTI, M.D., KITANO, T., TAGAWA, T., *et al.*, “Two small-crack extension force concept applied to fatigue limit of blunt notched components”, *International Journal of Fatigue*, v. 21, pp. 77–82, 1999.
- [18] ZERBST, U., SAVAIDIS, G., BEIER, H.T., “Special Issue on Fracture mechanics-based determination of the fatigue strength of weldments”, *Engineering Fracture Mechanics*, v. 198, pp. 1–208, 2018.

- [19] ZERBST, U., MADIA, M., SCHORK, B., *et al.*, *Fatigue and fracture of weldments. The IBESS approach for the determination of the fatigue life and strength of weldments by fracture mechanics analysis*. Cham: Springer, 2019.
- [20] TANAKA, K., AKINIWA, Y., “Resistance curve method for predicting propagation threshold of short fatigue cracks at notches”, *Engineering Fracture Mechanics*, v. 30, n. 6, pp. 863–876, 1988.
- [21] McEVILY, A.J., MINAKAWA, K., “Crack closure and the growth of short and long fatigue cracks”, *Scripta Metallurgica*, v. 18, n. 1, pp. 71–76, 1984.
- [22] McEVILY, J., EIFLER, D., MACHERAUCH, E., “An analysis of the growth of short fatigue cracks”, *Engineering Fracture Mechanics*, v. 40, n. 3, pp. 571–584, 1991.
- [23] McEVILY, J., “An analysis of the growth of small fatigue cracks”, *Materials Science and Engineering A*, v. 143, n. 1–2, pp. 127–133, 1991.
- [24] EL HADDAD, M.H., TOPPER, T.H., SMITH, K.N., “Prediction of non-propagating cracks”, *Engineering Fracture Mechanics*, v. 11, n. 3, pp. 573–584, 1979.
- [25] CHAPETTI, M.D., “Fatigue propagation threshold of short cracks under constant amplitude loading”, *International Journal of Fatigue*, v. 25, n. 12, pp. 1319–1326, 2003.
- [26] MILLER, K.J., “The short crack problem”, *Fatigue and Fracture of Engineering Materials and Structures*, v. 5, n. 3, pp. 223–232, 1982.
- [27] MOLINA, C.A., CHAPETTI, M.D., “Estimation of high cycle fatigue behaviour using a threshold curve concept”, *International Journal of Fatigue*, v. 108, pp. 47–52, 2018.
- [28] MAIERHOFER, J., GÄNSER, H.P., PIPPAN, R., “Modified Kitagawa-Takahashi diagram accounting for finite notch depths”, *International Journal of Fatigue*, v. 70, pp. 503–509, 2015.
- [29] GARB, C., LEITNER, M., STAUDER, B., *et al.*, “Application of modified Kitagawa-Takahashi diagram for fatigue strength assessment of cast Al-Si-Cu alloys”, *International Journal of Fatigue*, v. 111, pp. 256–268, 2018.
- [30] LEONETTI, D., MALJAARS, J., SNIJDER, H.H., “Fracture mechanics based fatigue life prediction for a weld toe crack under constant and variable amplitude random block loading – Modeling and uncertainty estimation”, *Engineering Fracture Mechanics*, v. 242, 107487, 2021.
- [31] MURAKAMI, Y., *Metal fatigue: Effect of Small Defects and Nonmetallic Inclusions*. 2 ed. Elsevier, 2019.
- [32] MURAKAMI, Y., ENDO, M., “Effects of defects, inclusions and inhomogeneities on fatigue strength”, *International Journal of Fatigue*, v. 16, n. 3, pp. 163–182, 1994.
- [33] SCHIJVE, J., *Fatigue of Structures and Materials*. Dordrecht: Springer, 2009.
- [34] FUCHS, H.O., “*Metal fatigue in engineering*”. 1 ed. New York: John Wiley and Sons, 1980.
- [35] THE BRITISH STANDARDS INSTITUTION (BSI). *BS 7910 Guide to methods for assessing the acceptability of flaws in metallic structures*. London: BSI, 2019.
- [36] KLESNIL, M., LUKÁŠ, P., *Fatigue of metallic materials*. 2 ed. Amsterdam: Elsevier, 1992. v. 7.
- [37] ZHENG, X., HIRT, M.A., “Fatigue crack propagation in steels”, *Engineering Fracture Mechanics*, v. 18, n. 5, pp. 965–973, 1983.
- [38] POURHEIDAR, A., PATRIARCA, L., MADIA, M., *et al.*, “Progress in the measurement of the cyclic R-curve and its application to fatigue assessment”, *Engineering Fracture Mechanics*, v. 260, 108122, 2022.
- [39] CASTRO, J.T.P., MEGGIOLARO, M.A., MIRANDA, A.C.O., *et al.*, “Prediction of fatigue crack initiation lives at elongated notch roots using short crack concepts”, *International Journal of Fatigue*, v. 42, pp. 172–182, 2012.
- [40] ABDEL-RAOUF, H., TOPPER, T.H., PLUMTREE, A., “A short fatigue crack model based on the nature of the free surface and its microstructure”, *Scripta Metallurgica et Materialia*, v. 25, pp. 597–602, 1991.
- [41] ABDEL-RAOUF, H., DUQUESNAY, D.L., TOPPER, T.H., *et al.*, “Notch-size effects in fatigue based on surface strain redistribution and crack closure”, *International Journal of Fatigue*, v. 14, n. 1, pp. 57–62, 1992.
- [42] CHAPETTI, M.D., KATSURA, N., TAGAWA, T., *et al.*, “Static strengthening and fatigue blunt-notch sensitivity in low carbon steels”, *International Journal of Fatigue*, v. 23, n. 3, pp. 207–214, 2001.
- [43] SANTUS, C., TAYLOR, D., “Physically short crack propagation in metals during high cycle fatigue”, *International Journal of Fatigue*, v. 31, n. 8–9, pp. 1356–1365, 2009.

- [44] GAËLLE C., CHRISTINE, S.B., LAURIE, L., *et al.*, “Near threshold fatigue propagation of physically short and long cracks in Titanium alloy”, *Procedia Structural Integrity*, v. 2, pp. 950–957, 2016.
- [45] KOÇAK, M., WEBSTER, S., JANOSCH, J., *et al.*, “FITNET, fitness-for-service procedure - Section 7: Fatigue module: Technical Report”, *European Fitness for Service Network*, 2006.
- [46] CHAPETTI, M.D., “Fracture mechanics for fatigue design of metallic components and small defect assessment”, *International Journal of Fatigue*, v. 154, 106550, 2022.
- [47] CHAPETTI, M.D., GUERRERO, A.O., “Estimation of notch sensitivity and size effect on fatigue resistance”, *Procedia Engineering*, v. 66, pp. 323–333, 2013.
- [48] STEIMBREGER, C., CHAPETTI, M.D., “Fatigue stress assessment of butt-welded joints with undercuts”, *International Journal of Fatigue*, v. 105, pp. 296–304, 2017.
- [49] STEIMBREGER, C., CHAPETTI, M.D., “Fracture mechanics based prediction of undercuts tolerances in industry”, *Engineering Fracture Mechanics*, v. 211, pp. 32–46, 2019.